

Spin-torque oscillator based on tilted magnetization of the fixed layer

Yan Zhou,^{*} C. L. Zha, S. Bonetti, J. Persson, and Johan Åkerman[†]

*Department of Microelectronics and Applied Physics,
Royal Institute of Technology, Electrum 229, 164 40 Kista, Sweden*

(Dated: November 7, 2018)

Abstract

The spin torque oscillator (STO), where the magnetization of the fixed layer is tilted out of the film plane, is capable of strong microwave signal generation in zero magnetic field. Through numerical simulations of the Landau-Lifshitz-Gilbert-Slonczewski equations, within a macro-spin approximation, we study the microwave signal generation as a function of drive current for two realistic tilt angles. The tilt magnetization of the fixed layer can be achieved by using a material with high out-of-plane magnetocrystalline anisotropy, such as $L1_0$ FePt.

^{*}Electronic address: zhouyan@kth.se

[†]Electronic address: akerman1@kth.se

Broadband microwave oscillators, such as e.g. the Yttrium Iron Garnet (YIG) oscillator, play an important role in communication, radar applications and high-precision instrumentation. The two major drawbacks of the YIG oscillator is its bulk nature (e.g. 1 mm YIG crystal spheres), which foils any attempt of monolithic integration, and its magnetic tuning, which is both complicated and consumes high power. The Spin Torque Oscillator [1, 2, 3, 4, 5, 6] may be thought of as a modern nanoscopic analog of the YIG oscillator: It is extremely broad band (multi octave), can achieve high spectral purity, and is magnetically tunable with a similar transfer function related to ferromagnetic resonance. While the STO has significant advantages, such as easy on-chip integration and *current* tunability, it typically requires a large static magnetic field for operation.

Various attempts have been made to realize STOs operating in the absence of an applied magnetic field. Originally suggested by Redon et.al. [7, 8], a perpendicularly polarized fixed layer may drive an in-plane magnetization into an out-of-plane precessional state even in the absence of an applied field. Zero-field operation was indeed recently experimentally demonstrated by Houssameddine *et al.* [9] using an STO with a perpendicularly polarized Co/Pt multilayer as fixed layer. However, due to the axial symmetry of the fixed layer magnetization and the precession, their STO requires an additional exchange biased read-out layer on top of the free layer to break the symmetry and generate any signal. The additional read out and exchange biasing layer complicates the structure and its fabrication. The signal quality is so far also quite limited compared to conventional STOs. A different solution was first suggested by Xiao *et al.* [10] and later developed in detail by Barnas *et al.* [11]. Their suggested STO is based on a wavy angular dependence of the spin torque, obtained by judiciously choosing free and fixed layer materials with different spin diffusion lengths. Boulle *et al.* recently fabricated such a wavy STO and demonstrated current tunable microwave generation in zero field [12]. Again, the output signal is quite limited, partly caused by the associated asymmetric magnetoresistance. A radically different approach was taken by Pribiag *et al.*, who introduced a magnetic vortex in a *thick* free layer and were able to excite zero-field gyromagnetic precession of the magnetic vortex core through the spin torque action from a conventional fixed layer [13]. While the signal quality of this vortex-STO is excellent, its frequency range is quite limited, so far only demonstrated below 3 GHz.

In this letter, a novel *Tilted-Polarizer* STO structure (TP-STO) has been studied where the fixed layer magnetization (\mathbf{M}) is tilted out of the film plane. In the reference frame of

the in-plane free layer magnetization (\mathbf{m}), the spin polarization hence has both in-plane components (p_x, p_y) and a component along the out-of-plane direction (p_z). We show that p_z can drive the free layer into precession *without* the need for an applied field, while the in-plane component M_x of the fixed layer magnetization generates a large magnetoresistance (MR), i.e. an rf output *without* the need for an additional read-out layer. While \mathbf{M} may have any out-of-plane direction in the general situation, we limit our discussion to the x - z plane, $\mathbf{M}=(M_x, 0, M_z)=|\mathbf{M}|(\cos \beta, 0, \sin \beta)$, and $\beta=36^\circ$ and 45° (Fig. 1), since these two particular angles can be achieved using different crystallographic orientations of FePt.

The time-evolution of the free layer magnetization \hat{m} is found using the standard Landau-Lifshitz-Gilbert-Slonczewski (LLGS) equation,

$$\frac{d\hat{m}}{dt} = -\gamma\hat{m} \times \mathbf{H}_{eff} + \alpha\hat{m} \times \frac{d\hat{m}}{dt} + \frac{\gamma}{\mu_0 M_{S,free}} \tau, \quad (1)$$

where \hat{m} is the unit vector of the free layer magnetization, $M_{S,free}$ its saturation magnetization, γ the gyromagnetic ratio, α the Gilbert damping parameter, and μ_0 the magnetic vacuum permeability. Setting the applied field to zero and separating the effect of the demagnetizing tensor into a positive anisotropy field along x , and a negative out-of-plane demagnetizing field we get $\mathbf{H}_{eff}=(H_k\hat{e}_x m_x - H_d\hat{e}_z m_z)/|\mathbf{m}|$. We define positive current as flowing from the fixed layer to the free layer. The quantity τ in Eq. 1 is the Slonczewski spin-transfer torque density,

$$\tau = \eta(\varphi) \frac{\hbar J}{2ed} \hat{m} \times (\hat{m} \times \hat{M}), \quad (2)$$

where φ is the angle between \hat{m} and \hat{M} , d is the free layer thickness, and

$$\eta(\varphi) = \frac{q_+}{A + B \cos(\varphi)} + \frac{q_-}{A - B \cos(\varphi)}. \quad (3)$$

where q_+ , q_- , A , B are all material dependent parameters [14]. In our simulations below we use Cu as spacer, Permalloy (Py) as the free layer, and FePt as the fixed layer. Due to the lack of available parameters for the Cu/FePt interface, we approximate $\eta(\varphi)$ in our Py/Cu/FePt stack using literature values for Py/Cu/Co [10, 11, 14, 15, 16, 17, 18]. This approximation may be justified if a thin polarizing layer of Co is used at the Cu/FePt interface.

We use the following generalized form for describing the angular dependence of MR [19, 20, 21, 22, 23, 24],

$$r = \frac{R(\varphi) - R_P}{R_{AP} - R_P} = \frac{1 - \cos^2(\varphi/2)}{1 + \chi \cos^2(\varphi/2)}, \quad (4)$$

where r is the reduced MR, χ is an asymmetry parameter describing the deviation from sinusoidal angular dependence, and R_P and R_{AP} denotes the resistance in the parallel and antiparallel configurations respectively.

While both the asymmetric torque and the asymmetric magnetoresistance are derived for in-plane spin polarizations and magnetizations, we argue that they will still hold as long as spin-orbit coupling is weak. While this is true for Py, it might still be questionable for FePt due to its large magnetocrystalline anisotropy. We argue that any deviation due to strong spin-orbit coupling will not change the general result of our study and is likely further weakened by our choice of a thin polarizing layer of Co on top of FePt.

Fig. 2a shows the precession frequency vs. drive current density for the two selected angles. We observe precession at both positive and negative current and the frequency increases with the magnitude of the current density, similar to perpendicularly polarized STOs [8, 25, 26]. As in simulations for perpendicularly polarized STOs [8], the precession starts along the equator and continues to follow increasing latitudes of the unit sphere throughout the entire frequency range (f increases due to the increasing demagnetizing field) until it reaches a static state at the north (south) pole for large negative (positive) current (Fig. 2c). We highlight six orbits (denoted by A, B, C, D, E, F) which correspond to points in Fig. 2a and 2b. \mathbf{m} precesses in the north hemisphere for negative J and in the south hemisphere for positive J in an attempt to align/anti-align with \mathbf{M} . We hence conclude that the precession is largely dominated by the perpendicular component p_z of the spin polarized current and virtually independent of the in-plane components. The asymmetry of the dependence for different current polarity is due to the asymmetric spin torque form as shown in the inset of Fig. 2a.

Fig. 2b shows the effective MR (MR_{eff}) as a function of current density for the two tilt angles and different choices of χ . $\text{MR}_{\text{eff}}J^2$ is a measure of the expected rf output where MR_{eff} is the difference between the maximum and minimum resistance values along the orbit normalized by the full $R_{AP}-R_P$. As the precession orbit contracts with increasing $|J|$, one may expect MR_{eff} to be maximum at the equator and exhibit a monotonic decrease with increasing $|J|$. While symmetric MR ($\chi=0$) indeed yields a maximum MR_{eff} at the onset of precession, the higher the MR asymmetry, the more the MR_{eff} peak gets shifted to higher positive current. For asymmetric angular dependence of MR, it is hence favorable to precess at a finite latitude with a larger average angle *w.r.t* to \mathbf{M} . For optimal output it is

consequently desirable to use positive currents and tailor χ as to position MR_{eff} in the middle of the operating frequency range. While there are no χ values reported for NiFe/Cu/FePt, χ may range from 0 to 4 in other trilayers involving NiFe [20, 22, 27, 28].

It is interesting to note that despite the large in-plane component of the spin polarization, the initial static states are virtually identical to the north and south poles where the spin torque and the torque from the demagnetizing field balance each other. However, if we further increase $|J|$ we expect this equilibrium point to move towards (anti)alignment with \hat{M} . As shown in Fig. 3, \hat{m} starts out at $\theta \approx 1^\circ$ and 177° and then gradually follows a curved trajectory to align with \hat{M} at very large negative current and anti-align at very large positive current. The resistance will change accordingly and at very large currents reach R_P and R_{AP} respectively.

There are several experimental ways to achieve easy-axis tilted hard magnets [29, 30, 31, 32, 33, 34]. For example, an easy axis orientation of 36° can be achieved by growing $L1_0$ (111) FePt on conventional Si (001) substrate [33] or on MgO(111) underlayer [34]. The 45° orientation can be achieved by epitaxially growing an $L1_0$ (101) FePt thin film on a suitable seed layer (e.g. CrW (110) with bcc lattice) at a temperature above $T=350^\circ\text{C}$ [29]. $L1_0$ FePt has high magnetocrystalline anisotropy ($K_u=7\times 10^7$ erg/cm³), high saturation magnetization ($M_s=1140$ emu/cm³), and a high Curie temperature ($T_c=750$ K). In both cases, a thin Co layer may be deposited on top of the fixed layer to promote a high degree of spin polarization. This is then followed by a standard Cu spacer and a NiFe free layer.

In summary, the Tilted-Polarizer STO structure (TP-STO), where the fixed layer has a tilted out-of-plane oriented magnetization, yields the combined advantage of zero-field operation and high output signal without the need for an additional sensing layer. Both the precession and effective MR dependence on the driving current and the equilibrium states of the STO can be well understood by investigating the precession orbits of the free layer. The TP-STOs with tilt angles $\beta=36^\circ$ and 45° can be fabricated by using FePt with high anisotropy and tilted easy-axis.

We thank M. Stiles for useful discussions. Support from The Swedish Foundation for strategic Research (SSF), The Swedish Research Council (VR), and the Göran Gustafsson Foundation is gratefully acknowledged.

-
- [1] J. C. Slonczewski, J. Magn. Magn. Mater. **159**, 1 (1996).
- [2] L. Berger, Phys. Rev. B **54**, 9353 (1996).
- [3] J. A. Katine, F. J. Albert, R. A. Buhrman, E. B. Myers, and D. C. Ralph, Phys. Rev. Lett. **84**, 3149 (2000).
- [4] S. I. Kiselev, J. C. Sankey, I. N. Krivorotov, N. C. Emley, R. J. Schoelkopf, R. A. Buhrman, and D. C. Ralph, Nature **425**, 380 (2003).
- [5] W. H. Rippard, M. R. Pufall, S. Kaka, S. E. Russek, and T. J. Silva, Phys. Rev. Lett. **92**, 027201 (2004).
- [6] I. N. Krivorotov, N. C. Emley, J. C. Sankey, S. I. Kiselev, D. C. Ralph, and R. A. Buhrman, Science **307**, 228 (2005).
- [7] O. Redon, B. Dieny, and B. Rodmacq, U.S. Patent No. 6532164 B2 (2003).
- [8] K. J. Lee, O. Redon, and B. Dieny, Appl. Phys. Lett. **86**, 022505 (2005).
- [9] D. Houssameddine, U. Ebels, B. Delaet, B. Rodmacq, I. Firastrau, F. Ponthenier, M. Brunet, C. Thirion, J.-P. Michel, L. Prejbeanu-Buda, et al., Nat. Mater. **6**, 447 (2007).
- [10] J. Xiao, A. Zangwill, and M. D. Stiles, Phys. Rev. B **70** (2004).
- [11] J. Barnas, A. Fert, M. Gmitra, I. Weymann, and V. K. Dugaev, Phys. Rev. B **72**, 024426 (2005).
- [12] O. Boulle, V. Cros, J. Grollier, L. G. Pereira, C. Deranlot, F. Petroff, G. Faini, J. Barnas, and A. Fert, Nat. Phys. **3**, 492 (2007).
- [13] V. S. Pribiag, I. N. Krivorotov, G. D. Fuchs, P. M. Braganca, O. Ozatay, J. C. Sankey, D. C. Ralph, and R. A. Buhrman, Nat. Phys. **3**, 498 (2007).
- [14] J. Xiao, A. Zangwill, and M. D. Stiles, Phys. Rev. B **72**, 014446 (2005).
- [15] J. Barnas, A. Fert, M. Gmitra, I. Weymann, and V. K. Dugaev, Mater. Sci. Eng. B **126**, 271 (2006).
- [16] M. Gmitra and J. Barnas, Phys. Rev. Lett. **99**, 097205 (2007).
- [17] M. Gmitra and J. Barnas, Appl. Phys. Lett. **89**, 223121 (2006).
- [18] M. Gmitra and J. Barnas, Phys. Rev. Lett. **96**, 207205 (2006).
- [19] J. Slonczewski, J. Magn. Magn. Mater. **247**, 324 (2002).
- [20] I. N. Krivorotov, D. V. Berkov, N. L. Gorn, N. C. Emley, C. Sankey, D. C. Ralph, and R. A.

- Buhrman, Phys. Rev. B **76**, 024418 (2007).
- [21] M. D. Stiles and A. Zangwill, J. Appl. Phys. **91**, 6812 (2002).
 - [22] S. Urazhdin, R. Loloee, and W. P. Pratt, Phys. Rev. B **71**, 100401 (2005).
 - [23] P. Dauguet, P. Gandit, J. Chaussy, S. F. Lee, A. Fert, and P. Holody, Phys. Rev. B **54**, 1083 (1996).
 - [24] A. Vedyayev, N. Ryzhanova, B. Dieny, P. Dauguet, P. Gandit, and J. Chaussy, Phys. Rev. B **55**, 3728 (1997).
 - [25] X. Zhu and J. G. Zhu, IEEE Trans. Magn. **42**, 2670 (2006).
 - [26] W. Jin, Y. W. Liu, and H. Chen, IEEE Trans. Magn. **42**, 2682 (2006).
 - [27] N. Smith, J. Appl. Phys. **99** (2006).
 - [28] A. Shpiro, P. M. Levy, and S. F. Zhang, Phys. Rev. B **67** (2003).
 - [29] B. Lu and D. Welle, U.S. Patent No. 0009766 A1 (2007).
 - [30] J. P. Wang, W. K. Shen, J. M. Bai, R. H. Victora, J. H. Judy, and W. L. Song, Appl. Phys. Lett. **86**, 142504 (2005).
 - [31] Y. F. Zheng, J. P. Wang, and V. Ng, J. Appl. Phys. **91**, 8007 (2002).
 - [32] T. J. Klemmer and K. Pelhos, Appl. Phys. Lett. **88**, 162507 (2006).
 - [33] C. L. Zha, B. Ma, Z. Z. Zhang, T. R. Gao, F. X. Gan, and Q. Y. Jin, Appl. Phys. Lett. **89**, 022506 (2006).
 - [34] J. Y. Jeong, J. G. Kim, S. Y. Bae, and K. H. Shin, IEEE Trans. Magn. **37**, 1268 (2001).

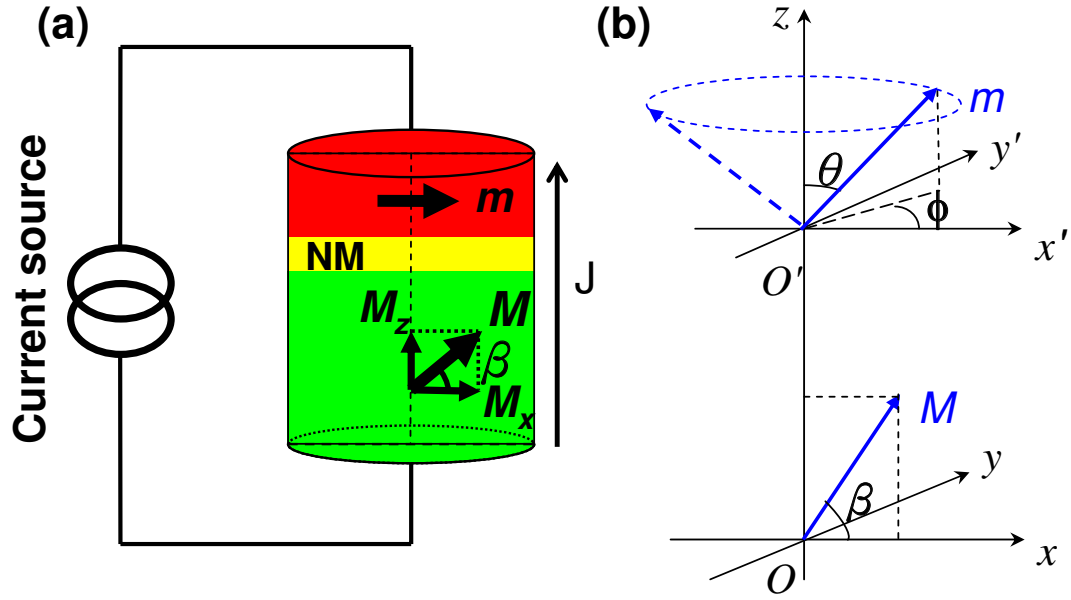


FIG. 1: (a) schematic of a TP-STO. \mathbf{M} is the fixed layer magnetization with tilted orientation. The free layer magnetization \mathbf{m} is separated from the fixed layer by a nonmagnetic layer (NM); (b) the coordinate system used in this work. \mathbf{M} lies in the x - z plane with angle β *w.r.t.* the x -axis.

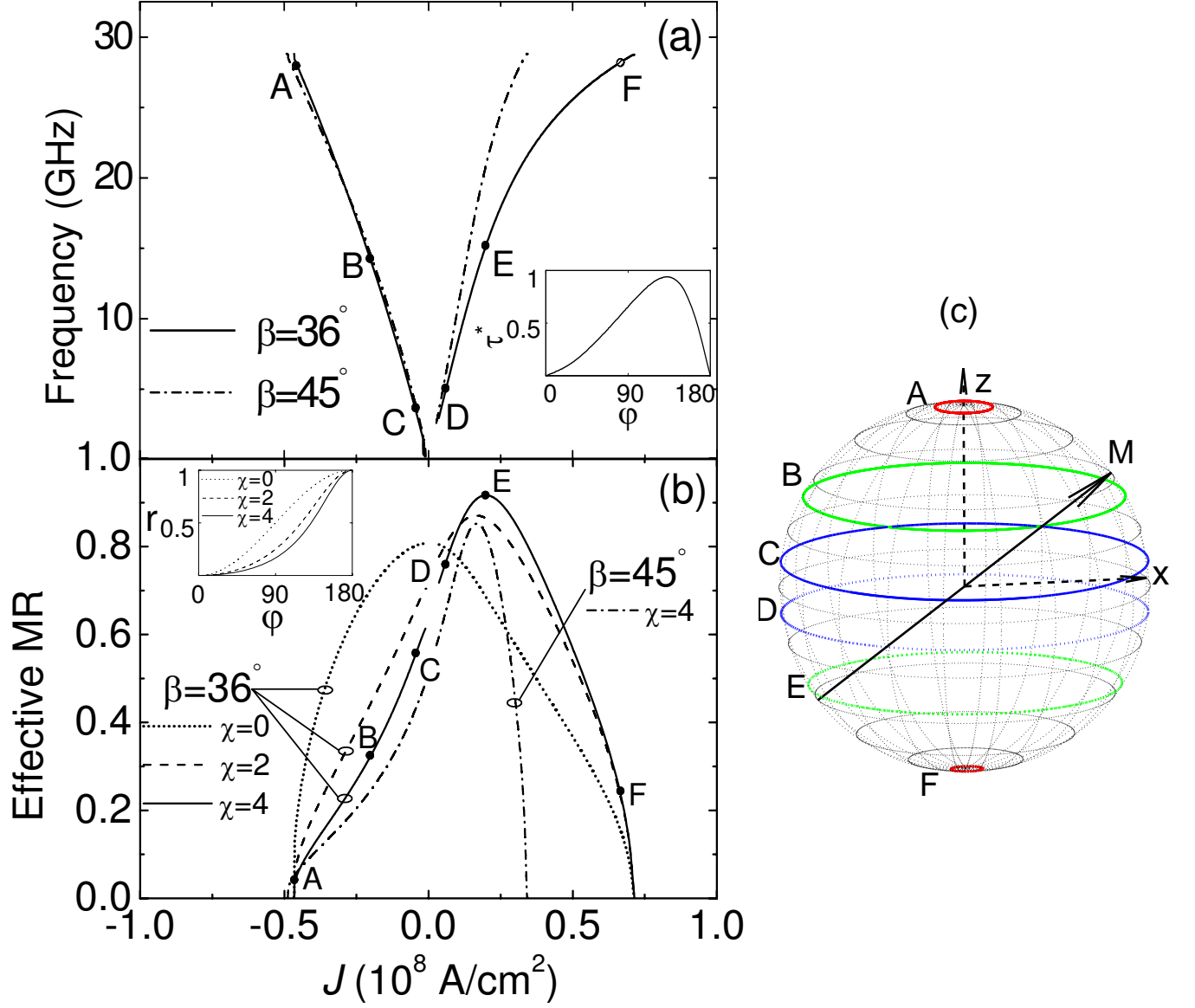


FIG. 2: (a) Precession frequency vs. drive current for $\beta=36^\circ$ (solid line) and $\beta=45^\circ$ (dash dot line). Inset: Normalized spin torque $\tau^*=4ed\tau/\hbar J$ vs. φ . (b) Effective MR vs. J for $\beta=36^\circ$ (solid line) and $\beta=45^\circ$ (dashed line). Inset: Reduced MR vs. φ . (c) Precession orbits on the unit sphere for different J and $\beta=36^\circ$.

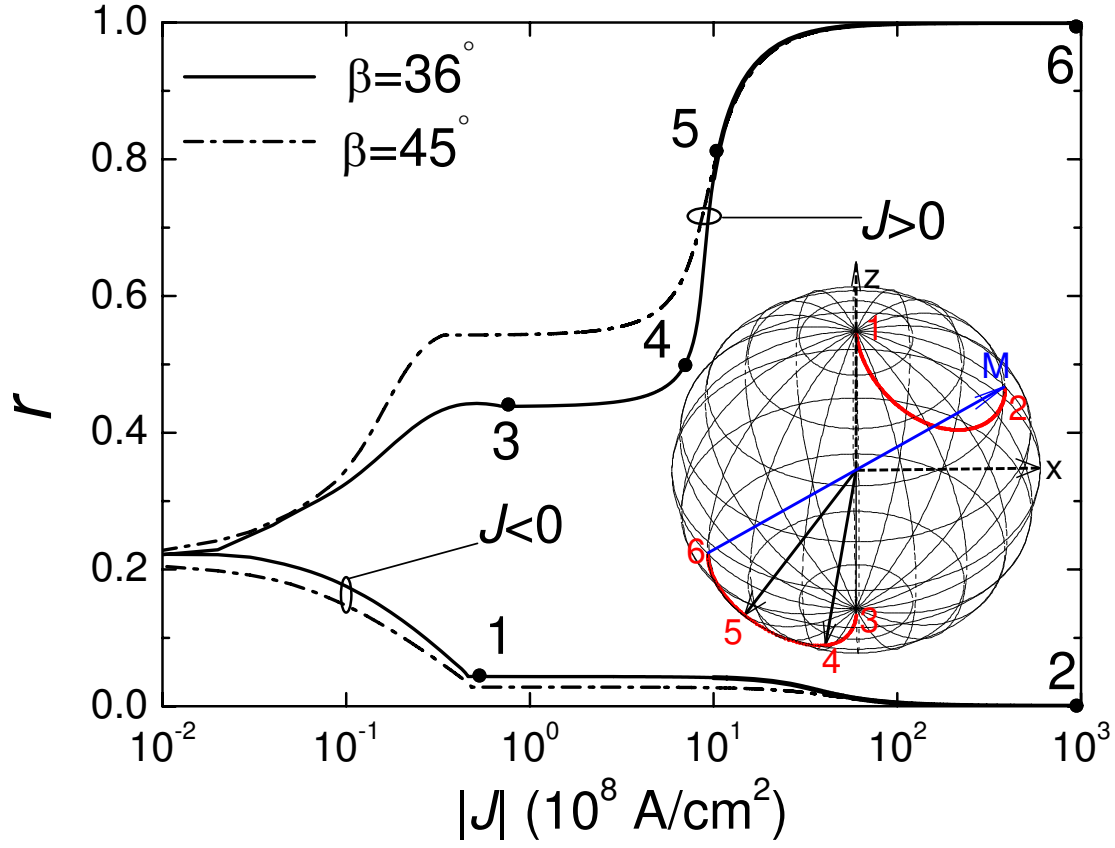


FIG. 3: Magnetoresistance as a function of current density. Inset: the equilibrium states of \hat{m} at different current densities when $\beta = 36^\circ$. 1: $J = -0.5 \times 10^8 \text{ A/cm}^2$; 2: $J = -1 \times 10^{11} \text{ A/cm}^2$; 3: $J = 0.75 \times 10^8 \text{ A/cm}^2$; 4: $J = 7 \times 10^8 \text{ A/cm}^2$; 5: $J = 1 \times 10^9 \text{ A/cm}^2$; 6: $J = 1 \times 10^{11} \text{ A/cm}^2$.